RESEARCH ARTICLE

Effect of Li doping on the structural, electronic and magnetic properties of Mn(N, As)

Monir Kamalian[1,*], Abdus Salam Sepahi[2], Zeinab Moradi[3]

[1] Department of physics, Yadegar-e-Imam Khomeini (RAH) Shahre-Rey Branch, Islamic Azad University, Tehran, Iran.

[2] Department of physics, Ferdowsi University of Mashhad, Mashhad, Iran.

[3] Faculty of physics, K. U. Toosi University of Technology, Tehran, Iran.

ARTICLE INFO

Article History:
Received 2021-08-01
Accepted 2021-10-20
Published 2021-11-01

Keywords:
Density Functional Theory (DFT)
LiMn(N, As)
Spintronic
Quantum ESPRESSO

ABSTRACT

In this study the effect of Li doping on the structural, electronic and magnetic properties of Mn(N, As) compounds was investigated using the Density Functional Theory (DFT) with the Quantum ESPRESSO software. The effect of the Li impurity on the Mn(N, As) conduction behavior and physical characteristics such electronic band structure and density of states (DOS) were considered and discussed simultaneously. The obtained results demonstrated that after Li doping, the equilibrium lattice constant (a0) was decreased and the band gap energy was increased. The electronic band structure and density of states (DOS) of the MnN compound showed the metallic and anti-ferromagnetic characteristics while the MnAs compound exhibited the half-metallic and ferromagnetic properties,however, by adding the Li impurity to these compounds, semiconducting and anti-ferromagnetic characteristics were observed. Moreover, the high spin configuration of the Mn atoms at thee DOS profiles revealed that these two anti-ferromagnetic compounds might also be promising candidates for future magneto-electronic and spintronic devices such as resonant tunneling magnetoresistance, ultrafast and ultrahigh-density spintronic devices.

How to cite this article
*Kamalian M., Salam Sepahi A., Moradi Z. Effect of Li doping on the structural, electronic and magnetic properties of Mn(N, As). J. Nanoanalysis., 2021; 8(4): -7. DOI: 10.22034/jna.***.*

INTRODUCTION

Transition metal nitrides have recently attracted much attention due to their excellent structural, optical, electronic, and magnetic properties that can be applied to many fields, including optical and wear-resistant coatings, magnetic recording and sensing, giant magnetoresistance (GMR) and tunneling magnetoresistance (TMR) devices and spintronics such as spin field effect transistors, spin valves, spin qubits, electro-optical switches, spin injector and ultra-sensitive magnetic field sensors [1-10]. Transition metals are always of immense interest to the researchers for their magnetic properties due to their unfilled d-orbitals. Mn-N compound is the interest for a number reasons such as the novel structural, chemical stability and interesting magnetic and optical properties [11, 12]. Due to these properties the MnN is of great current interest in theoretical and experimental studies and in practical applications [13]. In fact, no investigations have been reported on alkali elements as dopants to substitute Mn-sites in MnN. Hence, we choose Li as a dopant atom. It is expected that lithium dopant could markedly affect the structural and magnetic properties of LiMnN. Beside the family of half-metallic compounds such as MnAs is a promising candidate for magneto-electronic and spintronic devices because of the large carrier spin polarization, relatively high saturation magnetization and resonant tunneling magnetoresistance [14-16]. One promising candidate material for new spintronic applications is LiMnAs, given its suitable band gap and high magnetic moment per Mn atom [17-18]. It offers a good starting point for the development of novel

* Corresponding Author Email: *M.kamalian@srbiau.ac.ir*

semiconducting magnetic materials for applications in devices such as single-electron transistors [19].

In this paper, we investigated a comparative *ab initio* study for the structural, electronic and magnetic properties between the zinc-blende pure and doped MnN and MnAs with Li impurities within the density functional theory.

COMPUTATIONAL METHODS

Our calculations were performed within the framework of the Density Functional Theory (DFT), as implemented in the Quantum ESPRESSO computational code [20]. The electron exchange and correlation were treated according to the generalized gradient approximation (GGA) with the Perdew Burke Ernzerhof (PBE) gradient-corrected functional [21]. The Kohn-Sham equations were solved with flat waves: also, the use was made of ultra-soft pseudopotentials for the manganese, nitrogen, Arsenide and lithium atoms. The cutting energy of 50 Ry was taken to the flat waves. Our all structures have a size 10´10´10 of the unit cells. Brillouin-zone integrations were performed using the Monkhorst–Pack scheme [22] with a grid size of 10´10´10 for structural optimization and total energy calculation. The k-point size was selected to 10´10´10 to get the electronic band dispersion curve. In order to obtain band structures of these structures, the vc-relax, nscf and bands calculations have been performed subsequently. Finally, the density of states (DOS) has also been calculated to gain a view of the total electronic states. For calculating the density of states (DOS), we use a 20 × 20 × 20 grid size.

RESULTS AND DISCUSSION

Structural properties

We studied MnN and MnAs with the zinc-blend crystal structure, of which the unit cell was that of an fcc lattice with eight atoms. Fig. 1 shows the crystalline structure of both pure MnN and MnAs and these structures doped with the li atom.

Optimized geometric lattice parameters such as the equilibrium lattice constant (a) of all these proposed structures and the c/a ratio of LiMn(N, As) structures were calculated after the relaxation, as summarized in table I. The values of the optimized lattice constants for Zinc-blende Mn(N, As), (4.27 A°, 5.73 A°) were in a good agreement, as compared with the experimental values (4.30 A°, 5.71 A°) [23]. Adding the Li atom to Mn(N, As) decreased the equilibrium lattice constants, as observed.

Electronic properties

Electronic Band Structure

Fig.2 illustrates the electronic band structures of MnN and MnAs for both spin-up and spin-down

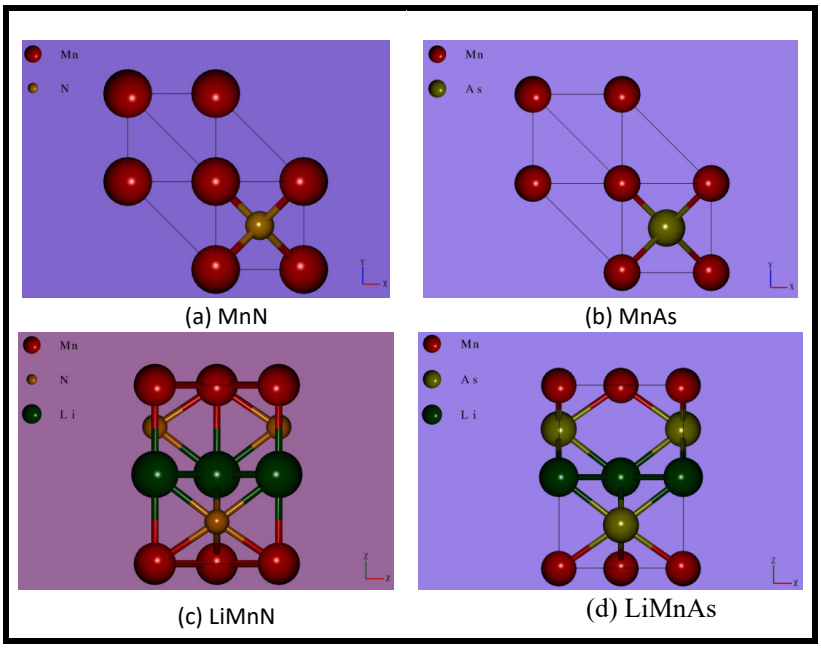

Fig. 1. schematic diagram of chosen unit cells of (a) MnN, (b) MnAs, (c) LiMnN and (d) LiMnAs.

Table 1. The calculated, optimized equilibrium lattice constant a (A°) and c/a ratio (A°) of the proposed structures.

Structure	Lattice constant a (A°)	c/a ratio (A°)
MnN	4.27	…..
MnAs	5.73	…..
LiMnN	3.45	1.43
LiMnAs	4.15	1.46

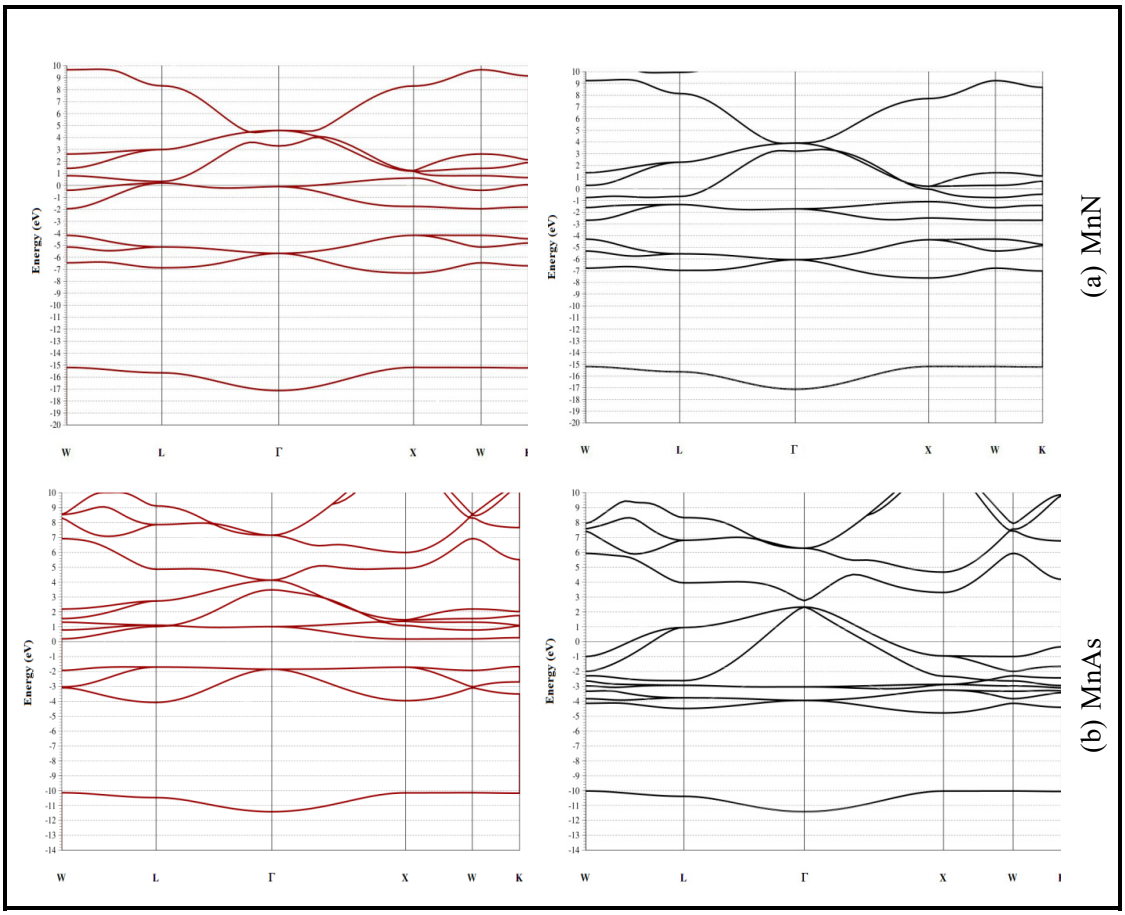

Fig. 2. Electronic band structure of (a) MnN (b) MnAs in the zinc-blende phase for spin-down at the left side and spin-up at the right side respectively. The energy zero is set at the Fermi energy.

along the high-symmetry path in the Brillouin zone. The energy zero was set at the Fermi energy.

Zero band gap energy in the G point of MnN for both spin-up and spin-down channels has been shown to exhibit metallic anti-ferromagnetic characteristics, whereas MnAs displayed a ferromagnetic half-metallic property. The splitting of the spin-up bands in the G point at the Fermi level was 0.39 eV. The valance band maximum and the conduction band minimum for both structures in the two spin-up and spin-down channels were situated in the same direction of the first brillouin zone; hence, these structures had the direct gap. The total magnetic moment of MnAs and MnN was 0 and 4 m_B respectively, corresponding to the predicated and experimental values [20]. It could be seen that total magnetic moment was raised as the lattice constant (a_0) was increased.

The electronic band structures of anti-ferromagnetic LiMnN and LiMnAs along the high-symmetry path in the Brillouin zone are shown in Fig.3. The energy zero was set at the Fermi energy.

The primitive unit cell of LiMn(N, As) contains two magnetic Mn atoms (Mn-I and Mn-II). As a

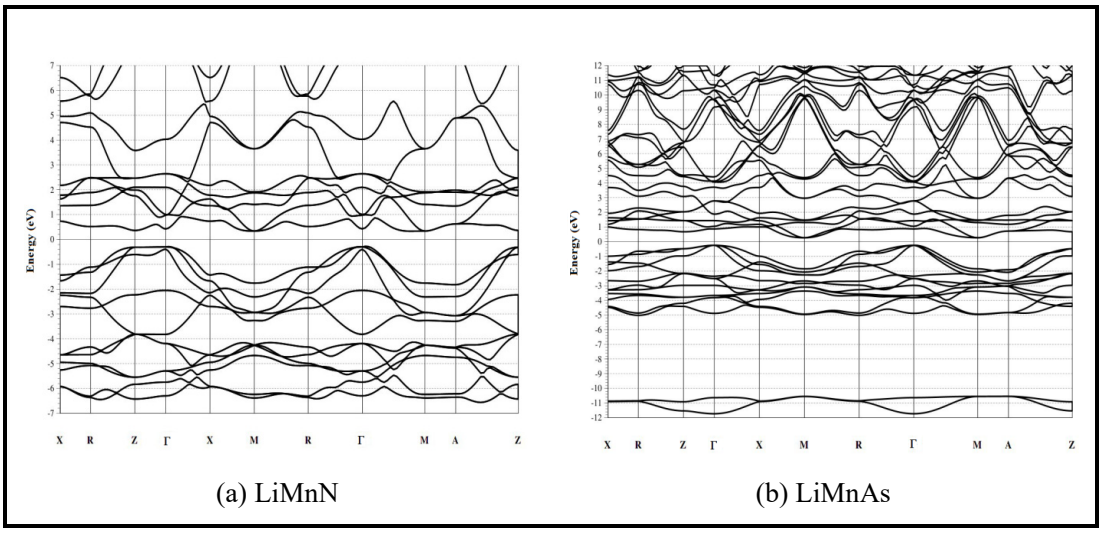

Fig. 3. Band structure of anti-ferromagnetic (a) LiMnN and (b) LiMnAs. The energy zero is set at the Fermi energy.

result the total magnetic moment (the integration of the spin-down and spin-up contribution) of these two atoms was zero. So, both two spin-up and spin-down channels of the band structures were similar due to the anti-ferromagnetic characterization of the LiMn(N, As) structures.

The non-zero value band gap of LiMnN and LiMnAs as a result of adding the Li atoms to these two primitive structures in both spin-up and spin-down channels could be clearly seen. Comparing the band structure of these two structures showed, that the width of the band gap of LiMnN (0.56 eV) was higher than that of LiMnAs (0.48 eV); also, an indirect band gap in the (M-G) direction could be observed in both band structures. These two structures were a narrow band gap semiconductor because Li gave up its electron, causing the conduction band edge in the semiconducting channel to be occupied; however, the width of the conduction band and valence band became smaller from LiMnAs to LiMnN. The width valance band maximum and conduction band minimum energies in both up and down spin channels for LiMnN were changed from 1.49 eV to 0.48 eV and 1.69 eV to 0.65 eV for LiMnAs respectively. Adding the Li atom to Mn (N, As) structures caused the increase of the band gap energy.

Density of states

Fig. 4 presents the spin polarized density of states (DOS) calculated for all proposed structures. The Fermi level was placed at the zero energy. All DOSs showed both kind of spin splitting.

The non-zero density of states at the Femi level in the DOS curve of MnN for the two spin channels indicated that this structure exhibited the metallic behavior. It could be seen that the density of states of the two spin channels was approximately aligned anymore; hence, this structure had an anti-ferromagnetic configuration. A half-metallic behavior for MnAs was predicted because the DOS of MnAs at spin-up states was metallic, with a significant DOS at the Fermi level, while the spin-down states had a semiconducting characteristic. Also, it could be seen that the density of states for the two spins was not aligned anymore, such that one spin population was larger than the other one; hence, this structure had a ferromagnetic configuration.

LiMn(N, As) DOSs showed that this structure could have a strongly suppressed density of state around the Fermi level, indicating the electronic structures of a semiconductor. Furthermore, the total DOS of MnN and LiMn(N, As) structures in both spin-up and spin-down channels were equal because the majority spin on one structure became the minority one on the other one; so, these structures indicated the anti-ferromagnetic characteristics.

For both LiMnN and LiMnAs structures, the DOS for Mn-I spin-up was completely filled, while the one for Mn-I spin-down was partially filled under the Fermi level but Mn-II had the opposite occupancy. Therefore, both Mn-I and Mn-II showed Mn with a high spin configuration. Also, the observed enhancement of the total DOS of

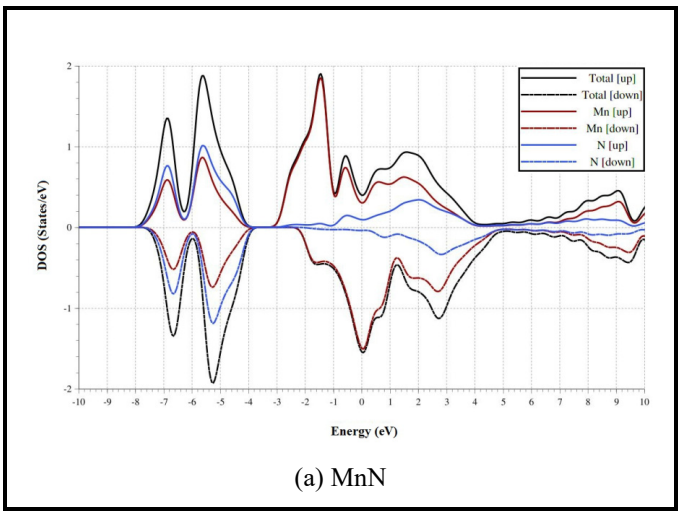

(a) MnN

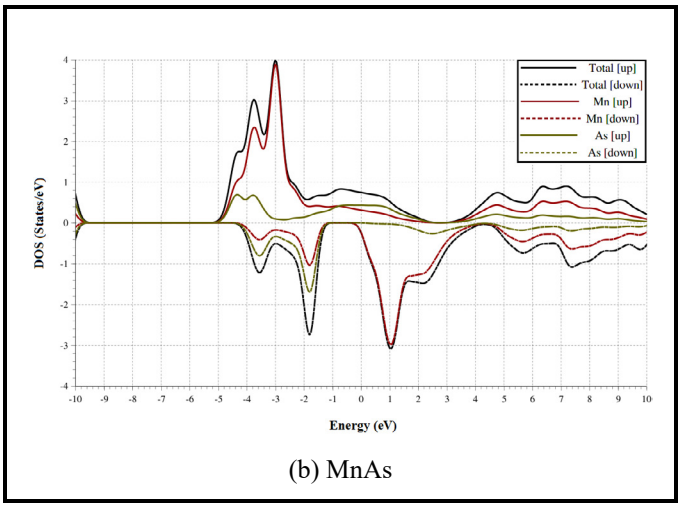

(b) MnAs

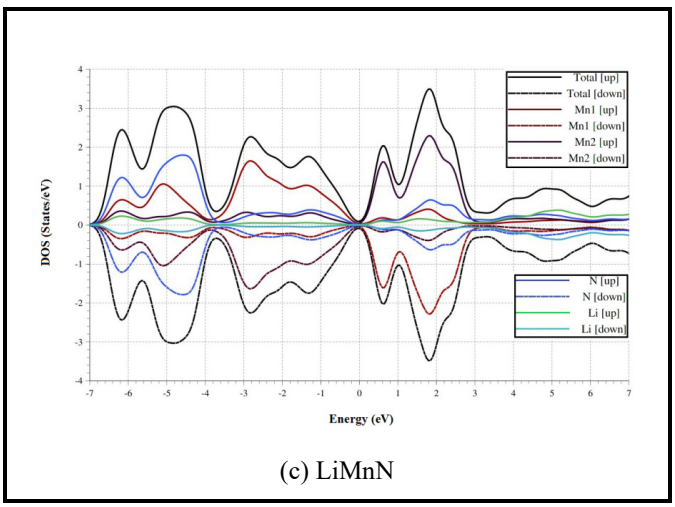

(c) LiMnN

Fig. 4. The calculated spin polrized density of state (DOS) curves of (a) MnN, (b) MnAs, (c) LiMnN and (d) LiMnAs for both two spin-up and down-spin channel are shown. The spin-up DOSs are plotted upwards while spin-down DOSs are plotted downwards. The horizontal dotted line at zero indicates the Fermi energy level.

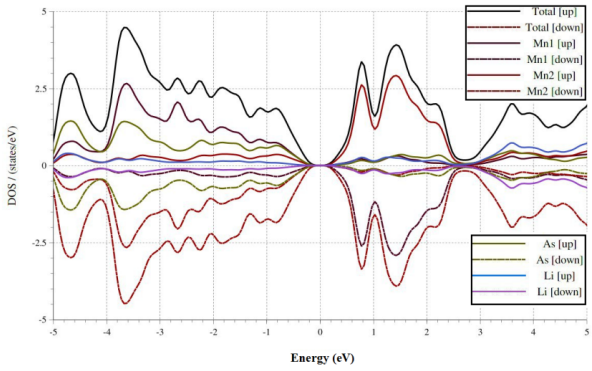

(d) LiMnAs

Continiued Fig. 4. The calculated spin polrized density of state (DOS) curves of (a) MnN, (b) MnAs, (c) LiMnN and (d) LiMnAs for both two spin-up and down-spin channel are shown. The spin-up DOSs are plotted upwards while spin-down DOSs are plotted downwards. The horizontal dotted line at zero indicates the Fermi energy level.

these two LiMnN and LiMnAs structures in the near Fermi level [-1eV to 1eV] indicated that DOS was modified by the Li atom incorporated into the pristine structures.

CONCLUSION

In this work, DFT calculation was used to investigate the effect of the Li doping on the structural, electronic and magnetic properties of Mn(N, As). The obtained results demonstrated that after doping Li, the equilibrium lattice constant was decreased and the band gap was increased. The electronic band structure and density of the state calculations also demonstrated MnN had a metallic and anti-ferromagnetic behavior while at least the G gap between the conduction band and the valance band in the channel spin-up MnAs represented the half-metallic and ferromagnetic behavior of this compound; however, Li doped Mn(N, As) displayed the semiconducting and anti-ferromagnetic characteristics. Furthermore, the high spin configuration of Mn-I and Mn-II at LiMn(N, As) could be of particular interest given the possible magneto-electronic and spintronic applications of these compounds.

CONFLICT OF INTEREST

The authors declare that there is no conflict of interest regarding the publication of this manuscript.

REFERENCE

[1] R. Yu, X. Chong, Y. Jiang, R. Zhou, W. Yuan, J. Feng, The stability, electronic structure, elastic and metallic properties of manganese nitrides, RSC Adv., 5, 1620 (2015).
[2] S. Salimian, S. Farjami shayesteh, J. Supercond. Nov. Magn., 25, 2009 (2012).
[3] W. J. Feng, N. K. Sun, J. Du, Q. Zhang, X. G. Liu, Y.F. Deng, Z. D. Zhang, Solid state Commun., 148, 199 (2008).
[4] R. Rajeswarapalanichamy, A. Amudhavalli, M. Manikandan, M. Kavitha, K. lyakutti, Phase Transitions., 90, 894 (2017).
[5] J. Sinclair, A. Hirohata, G. Vallejo-Fernandez, M. Meinert, K. O·Grady, J. Magn. Magn. Mater. 476, 278 (2018).
[6] P. Zilske, D. Graulich, M. Dunz, M. Meinert, Appl. Phys. Lett., 110, 192402 (2017).
[7] M. Kaminska, A. Twardowski, D. Wasik, J. Mater. Sci. Mater. Electron., 19, 828 (2008).
[8] M. Ribeiro, M. Marques, L. M. R. Scolfaro, L. K. Teles, L. G. Ferreira, AIP Conf. Proc. 893, 1227 (2007).
[9] M. Marques, L. K. Teles, L. M. R. Scolfaro, Appl. Phys. Lett., 86, 164105 (2005).
[10] R. S. Ningthoujam, N. S. Gajbhiye, Prog. Mater. Sci., 70, 50 (2015).
[11] J. Guerrero Sanchez, A. O. Mandru, K. Wang, N. Takeuchi, G. H. Cocoletzi, A. R. Smith, Appl. Surf. Sci, 355. 623 (2015).
[12] L. Alsaad, M. Bani Yassein, I. A. Qattan, A. Ahmad, S. R. Malkawi, Physica B Condens. Matter, 405, 1408 (2010).
[13] M. Dunz, T. Matalla-Wanger, M. Meinert, Phys. Rev. Research, 2, 013347 (2020).
[14] M. T. Elm, S. Hara, Advanced Materials, 26, 8079 (2014).
[15] E. D. Fraser, S. Hegde, L. SchWeidenback, A. H. Russ, A. Petrou, H. Luo, G. Kioseoglou, Appl. Phys. Lett., 97, 041103 (2010).
[16] R. Horiguchi, S. Hara, M. Lida, J. Appl. Phys., 124, 153905 (2018).
[17] T. Jungwirth, V. Novak, X. Matri, M. Cukr, F. Maca, A. B.

Shick, J. Masek, P. Horodyska, P. Nemec, B. L. Gallagher, R. P. Campion, C. T. Foxon, J. Wunderlich, Phys. Rev. B, 83, 035321 (2011).
[18] T. Jungwirth, X. Marti, P. Wadley, J. Wunderlich, Nat. Nanotechnol., 11, 231 (2016).
[19] J. Wunderlich, T. Jungwirth, B. Kaestner, A. C. Irvine, A. B. Shick, N. Stone, K. –Y. Wang, U. Rana, A. D. Giddings, C. T. Foxon, R. P. Campion, A. D. Williams, B. L. Gallagher, Phys. Rev. Lett., 97, 077201 (2006).
[20] P. Giannozi, S. Baroni, J. Phys. Condens. Matter, 21, 395502 (2009).
[21] J. P. Perdew, K. Burke, M. Ernzerohf, Phys. Rev. Lett. 77, 3865 (1996).
[22] H. J. Monkhorst , J. D. Pack, Phys. Rev. B, 13, 5188 (1976).
[23] R. De paiva, J. L. A. Alves, R. A. Nogueira, J. R. Leite, L. M. R. Scolfaro, Braz. J. Phys., 34, 568 (2004).